NASA TECHNICAL NOTE

NASA TN D-4209

NASA TN D-4209

PRELIMINARY EVALUATION OF XB-70 AIRPLANE ENCOUNTERS WITH HIGH-ALTITUDE TURBULENCE

by Eldon E. Kordes and Betty J. Love

Flight Research Center
Edwards, Calif.

NATIONAL AERONAUTICS AND SPACE ADMINISTRATION • WASHINGTON, D. C. • OCTOBER 1967

NASA TN D-4209

PRELIMINARY EVALUATION OF XB-70 AIRPLANE ENCOUNTERS WITH HIGH-ALTITUDE TURBULENCE

By Eldon E. Kordes and Betty J. Love

Flight Research Center
Edwards, Calif.

NATIONAL AERONAUTICS AND SPACE ADMINISTRATION

For sale by the Clearinghouse for Federal Scientific and Technical Information
Springfield, Virginia 22151 – CFSTI price $3.00

PRELIMINARY EVALUATION OF XB-70 AIRPLANE ENCOUNTERS WITH HIGH-ALTITUDE TURBULENCE

By Eldon E. Kordes and Betty J. Love
Flight Research Center

SUMMARY

Measurements of airplane response to clear-air turbulence were obtained during supersonic flights of the XB-70 airplanes to an altitude of 74,000 feet (22,555 meters) over the Western United States. In general, the results for 75,757 miles (121,919 kilometers) of operation above 40,000 feet (12,192 meters) altitude show that turbulence was encountered an average of 7.2 percent of the miles flown between 40,000 feet (12,192 meters) and 65,000 feet (19,812 meters) and an average of 3.3 percent of the miles flown above 65,000 feet (19,812 meters) with less than 1 percent of the turbulent areas exceeding 100 miles (160.93 kilometers) in length. Power-spectral-density estimates of the acceleration response to turbulence show that the structural modes contribute an appreciable amount to the total response.

INTRODUCTION

A great deal of flight information on the gust problem has been generated, as can be assessed from the extensive bibliography of reference 1. Almost all of this information is for flight altitudes below 40,000 feet (12,192 meters) and for subsonic flight velocities, with limited data at supersonic velocities of less than a Mach number of 2. In recent years, limited flight studies have been conducted to determine the nature and extent of turbulence for altitudes above 40,000 feet (12,192 meters) from VGH data (ref. 2) and from direct measurements of gust velocities (ref. 3). The objectives of designing and building large aircraft to fly at supersonic speeds at high altitudes have generated a need for more complete information on high-altitude turbulence.

Representative information on aircraft response to turbulence has been obtained during the flight-test program of the XB-70 airplane. Data on the response of the airplane have been recorded during 75,757 miles (121,919 kilometers) of flight at altitudes above 40,000 feet (12,192 meters) and Mach numbers above 1.0. This paper presents the results obtained so far in the program in terms of variation in percentage of rough air with altitude and in terms of sample power-spectral-density estimates of acceleration response to turbulence that are representative of a large airplane flying at supersonic speeds at high altitudes.

Symbols used in this paper are defined in appendix A. Measurements used in the investigation were taken in U. S. Customary Units and are given parenthetically in the

International System of Units (SI). The equivalent dimensions were determined by using the conversion factors in reference 4.

AIRCRAFT AND INSTRUMENTATION

The North American Aviation, Inc., XB-70 is a large, delta-wing, multiengine, jet airplane designed for supersonic cruise at a Mach number of 3 and altitudes above 70,000 feet (21,336 meters). Two airplanes were built, designated the XB-70-1 and XB-70-2. The three-view drawing of the XB-70-1 airplane in figure 1 shows the general configuration and overall dimensions. The basic design incorporates a thin, low-aspect-ratio wing with a 65.57° sweptback leading edge, folding tips, twin vertical stabilizers, and a movable canard with trailing-edge flaps. The XB-70-1 was manufactured with the wings mounted at a geometric dihedral angle of zero. The XB-70-2 wing was designed with 5° of positive dihedral. Geometric characteristics of the airplanes are given in table I; a more detailed description is presented in reference 5.

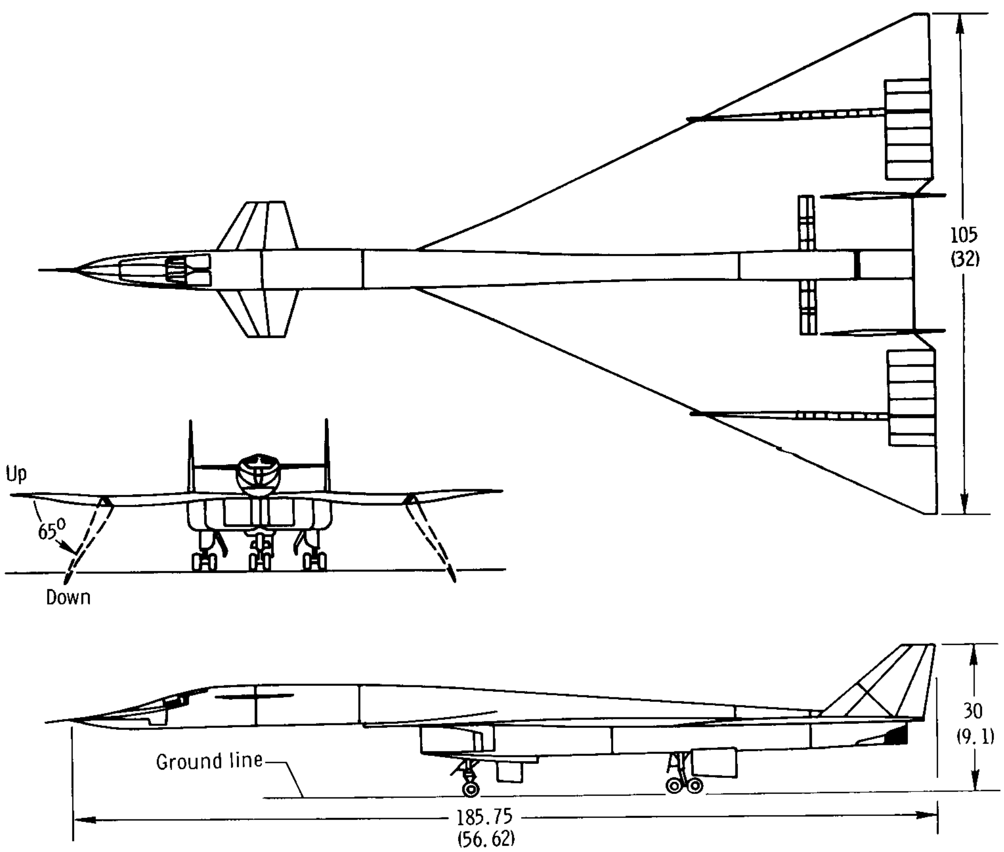

Figure 1.– Three-view drawing of XB-70-1 airplane. Dimensions in feet (meters).

The flight envelope covered during the 96-flight program is shown in figure 2; however, for the subject study only data above 40,000 feet and a Mach number of 1.0 were analyzed. For all flights above a Mach number of 1.4, the wing tips were folded down 65° (fig. 1).

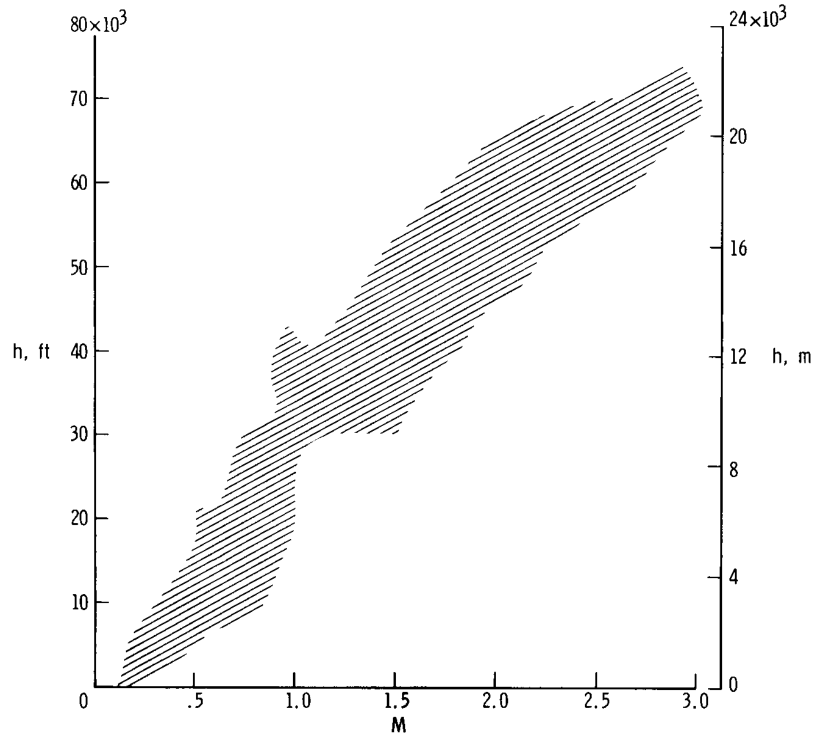

Figure 2.— Altitude—Mach number envelope of XB-70 flights.

During this investigation, continuous time histories of airspeed, pressure altitude, and normal acceleration at the airplane center of gravity and the pilot's station were recorded with a NASA VGH recorder (ref. 6). The data were recorded on photographic film that moved 14 inches per minute (0.0059 meter/second). In addition, analog signals of normal and lateral accelerations at the airplane center of gravity and at the pilot's station were recorded on magnetic tape of the XB-70 data system. This data system was capable of operation in either a continuous mode or in a sampling mode that recorded 6 seconds of data every 15 seconds. The mode of data recording was selected by the pilot for the particular flight-test condition of interest, and the time and duration of each record sample was indicated on the VGH film for coordination purposes. The basic characteristics and location of XB-70 data-system accelerometers pertinent to this study are listed in the following table:

Signal	Accelerometer range, g	Accuracy, percent full scale	Frequency range, cps	Location					
				Fuselage station		Butt plane		Water plane	
				in.	m	in.	m	in.	m
$a_{n_{cg}}$	±2	2.0	0 to 30	1485	37.72	11 right	0.28 right	-71	-1.80
$a_{y_{cg}}$	±1	2.0	0 to 30	1486	37.74	0 right	0 right	-37	-.94
$a_{n_{ps}}$	±5	2.0	0 to 30	438	11.13	12 right	.30 right	36	.91
$a_{y_{ps}}$	±2	2.0	0 to 30	442	11.23	12 right	.30 right	36	.91

Locations of the VGH accelerometers are presented in the table below:

Signal	Airplane	Location					
		Fuselage station		Butt plane		Water plane	
		in.	m	in.	m	in.	m
$a_{n_{cg}}$	No. 1	1480	37.59	0	0	-74.5	-1.89
	No. 2	1480	37.59	7 left	0.18 left	-74.5	-1.89
$a_{n_{ps}}$	No. 1	470	11.94	21 right	.53 right	25	.64
	No. 2	492	12.50	37 right	.94 right	36	.91

SCOPE OF FLIGHT TESTS

The flight measurements of airplane response were made during the first 96 flights of two XB-70 aircraft. Data on the response of the aircraft to clear-air turbulence were obtained during the general flight-test program. No attempt was made to seek turbulent conditions, although known areas of heavy turbulence were avoided. Data were obtained at altitudes above 40,000 feet (12,192 meters) and Mach numbers greater than 1.0. At Mach numbers greater than 1.4, the wing tips were folded in the full-down position and the windshield ramp was up.

All flights included in this study originated from Edwards Air Force Base, Calif., and were confined to the geographic area depicted in figure 3. Flight data were

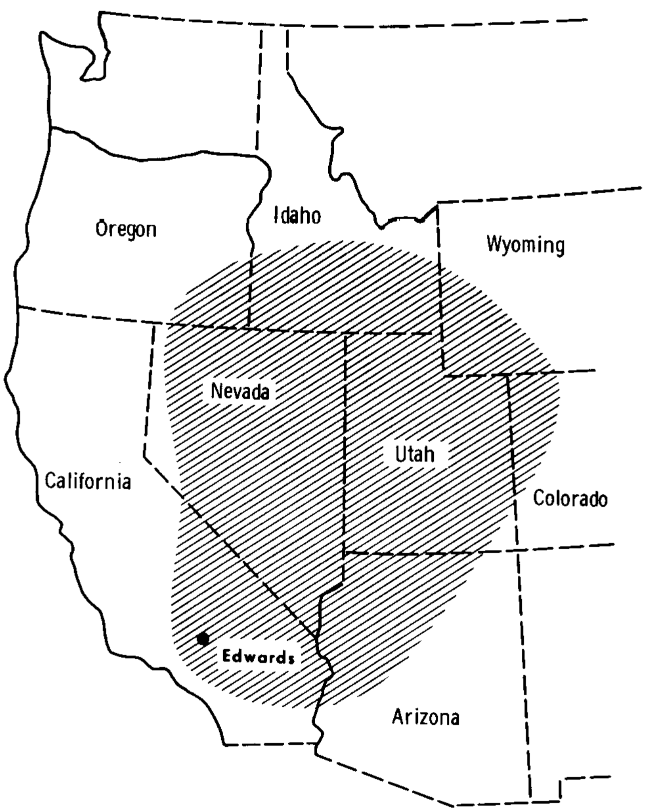

Figure 3.– Geographic area of XB-70 flights.

collected during all seasons over approximately 2 years. This study is concentrated on the airplane response for altitudes above 40,000 feet (12,192 meters) and at supersonic speeds.

EVALUATION OF DATA

The NASA VGH records were evaluated to obtain the percentage of rough air at various altitudes and the length (along the flight path) of the turbulent areas encountered. The evaluation procedures were similar to those used in references 1 to 3 and 7. In evaluating the records, a value of the threshold of peak accelerations was established as ±0.06g. Values of the derived gust velocity threshold for the delta-wing XB-70 were calculated as described in appendix B. These values were used to establish approximately the gust velocity thresholds and to assure that the results would include values of the derived gust velocity greater than 1.5 ft/sec (0.46 m/sec).

The length of turbulent areas and the percentage of miles in rough air were determined by considering the aircraft to be in rough air whenever the envelope of the incremental normal-acceleration trace remained greater than ±0.06g. In addition, the airspeed trace contained high-frequency fluctuations. The length of each turbulent area was obtained by multiplying the true airspeed (obtained from the Mach number and the speed of sound, ref. 8) by the time spent in rough air at each altitude interval. The summation of the lengths of the individual areas of rough air was divided by the total flight distance for the given altitude interval to obtain the percentage of rough air for each altitude interval.

For the analysis of airplane response, the data from the XB-70 flight recorder magnetic tape was first filtered by using a 20 cycle per second low-pass filter and then run through an analog-to-digital converter and recorded on digital-computer input tape. The cumulative frequency of acceleration was obtained by dividing the acceleration range into bands of 0.05g width and then programing the computer to count the number of times the accelerometer signal crossed the lower threshold of each band with positive slope. Data of 200 samples per second were used. The power spectral density of the acceleration response was computed by using the method of reference 9. Flight data of 50 samples per second and 100 lags were used. Since the flight recorder does not run continuously throughout the flight, data from many of the areas of interest were not available for computer analysis and only representative samples of data were obtained for a few conditions when the XB-70 recorder was in continuous operation at the time turbulence was encountered.

RESULTS AND DISCUSSION

Percentage of Flight Distances in Turbulence

A summary of the XB-70 gust experience during 57 flights which attained altitudes above 40,000 feet (12,192 meters) and supersonic speeds is presented in the following table for a threshold of ±0.06g:

Altitude range, ft	Altitude range, m	Distance flown, At altitude, miles	Distance flown, At altitude, km	Distance flown, In turbulence, miles	Distance flown, In turbulence, km	Percent of distance in turbulence
40,000 to 45,000	12,192 to 13,716	10,631	17,109	719	1157	6.8
45,000 to 50,000	13,716 to 15,240	7,958	12,807	571	919	7.2
50,000 to 55,000	15,240 to 16,764	9,264	14,909	658	1059	7.1
55,000 to 60,000	16,764 to 18,288	17,540	28,228	1306	2102	7.4
60,000 to 65,000	18,288 to 19,812	15,149	24,380	1100	1770	7.2
65,000 to 70,000	19,812 to 21,336	14,041	22,597	512	824	3.6
70,000 to 75,000	21,336 to 22,850	1,174	1,889	34	55	2.9
		75,757	121,919	4900	7886	6.4

The variation in percentage of distance in turbulence with altitude is shown in figure 4. In general, the data show that turbulence was encountered on an average of 7.2 percent of the miles between 40,000 feet (12,192 meters) and 65,000 feet (19,812 meters) and 3.3 percent of the miles above 65,000 feet (19,812 meters). For comparison, the results presented in reference 2 for flights of the U-2 over the Western United States are also shown. The XB-70 data indicate that large supersonic aircraft would be expected to encounter turbulence at high altitudes more often than predicted by the earlier data obtained from small subsonic aircraft. Some of the difference in the results of the two studies could be explained by the fact that the present investigation used an acceleration threshold of ±0.06g, whereas reference 2 used a derived gust velocity threshold of 2.0 ft/sec (0.610 m/sec). The major difference may be due, in part, to long wave length turbulence at high altitude. The long wave length turbulence

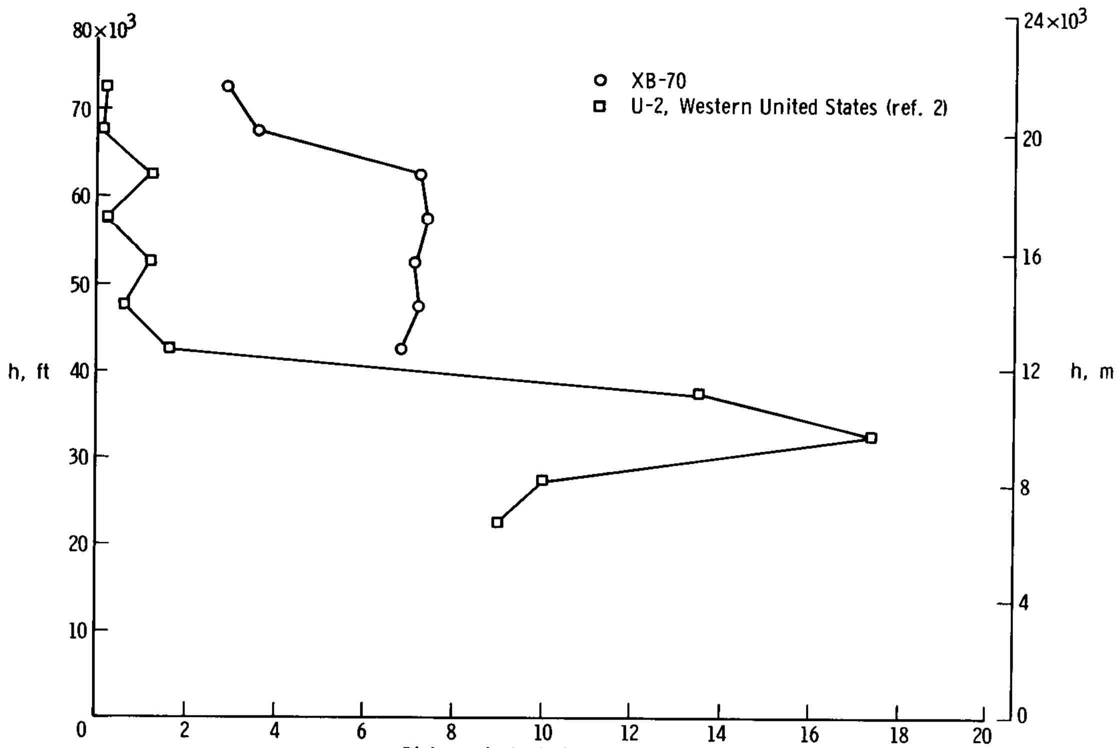

Figure 4.– Variation in percentage of distance in turbulence with altitude. Threshold $\Delta g_{cg} = \pm 0.06$.

would not be detected at low speed but would be significant at high speeds because of the effective gust frequency shift associated with the speed increase for given turbulence wave lengths. Flight results from the study of reference 3, in which an effort was made to measure turbulence reported by pilots of search aircraft and predicted by weather data, show that the measurement airplane was in turbulence about 10 percent of the search time above an altitude of 50,000 feet (15,240 meters).

Length of Turbulent Areas

The probability distribution of the length of the turbulent areas encountered above 40,000 feet (12,192 meters) altitude is shown in figure 5. The results show that the probability of exceeding a given length of turbulence decreases rapidly with increasing length of the turbulent area, with less than 1 percent of the turbulent areas exceeding 100 miles (160.93 kilometers). The largest turbulent area, 450 miles (724.2 kilometers), was encountered at an altitude between 60,000 feet (18,288 meters) and 65,000 feet (19,812 meters); the turbulent areas of approximately 200 miles (321.9 kilometers) were encountered at altitudes between 55,000 feet (16,764 meters) and 60,000 feet (18,288 meters). For comparison, the results presented in reference 2 for the Western United States are also shown in figure 5.

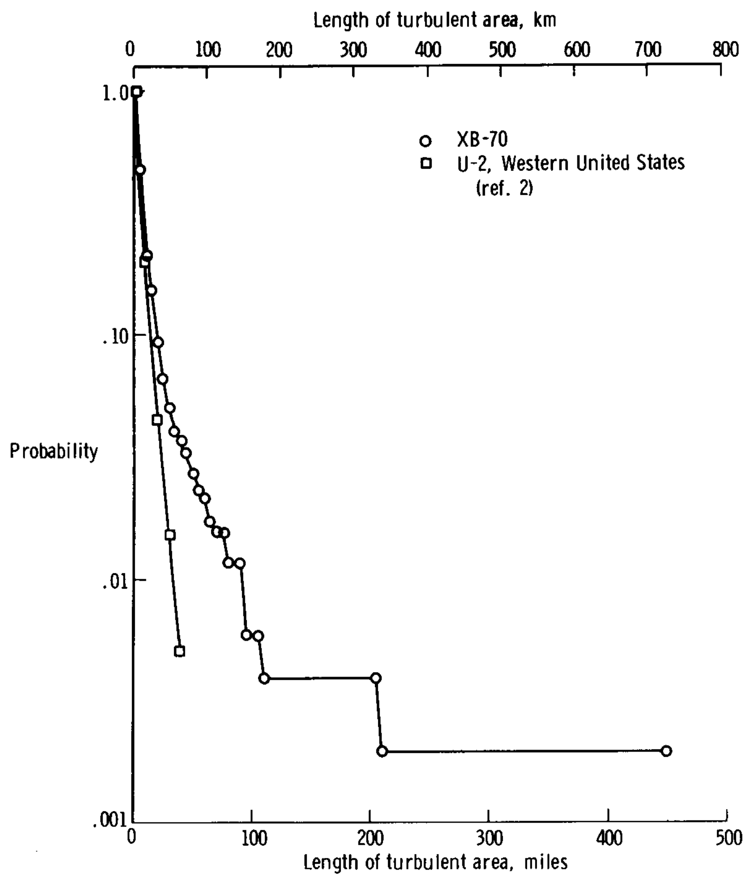

Figure 5.– Probability that turbulent area will exceed a given length.

Response to Turbulence

An example of the response of the XB-70 to clear-air turbulence at supersonic speed is shown in figure 6 in terms of the power-spectral-density estimates of normal and lateral accelerations at the center of gravity and at the pilot's station. These results are from 40 seconds of data taken at $M = 2.4$ and $h = 55,000$ feet (16,764 meters) with the flight augmentation control system on.

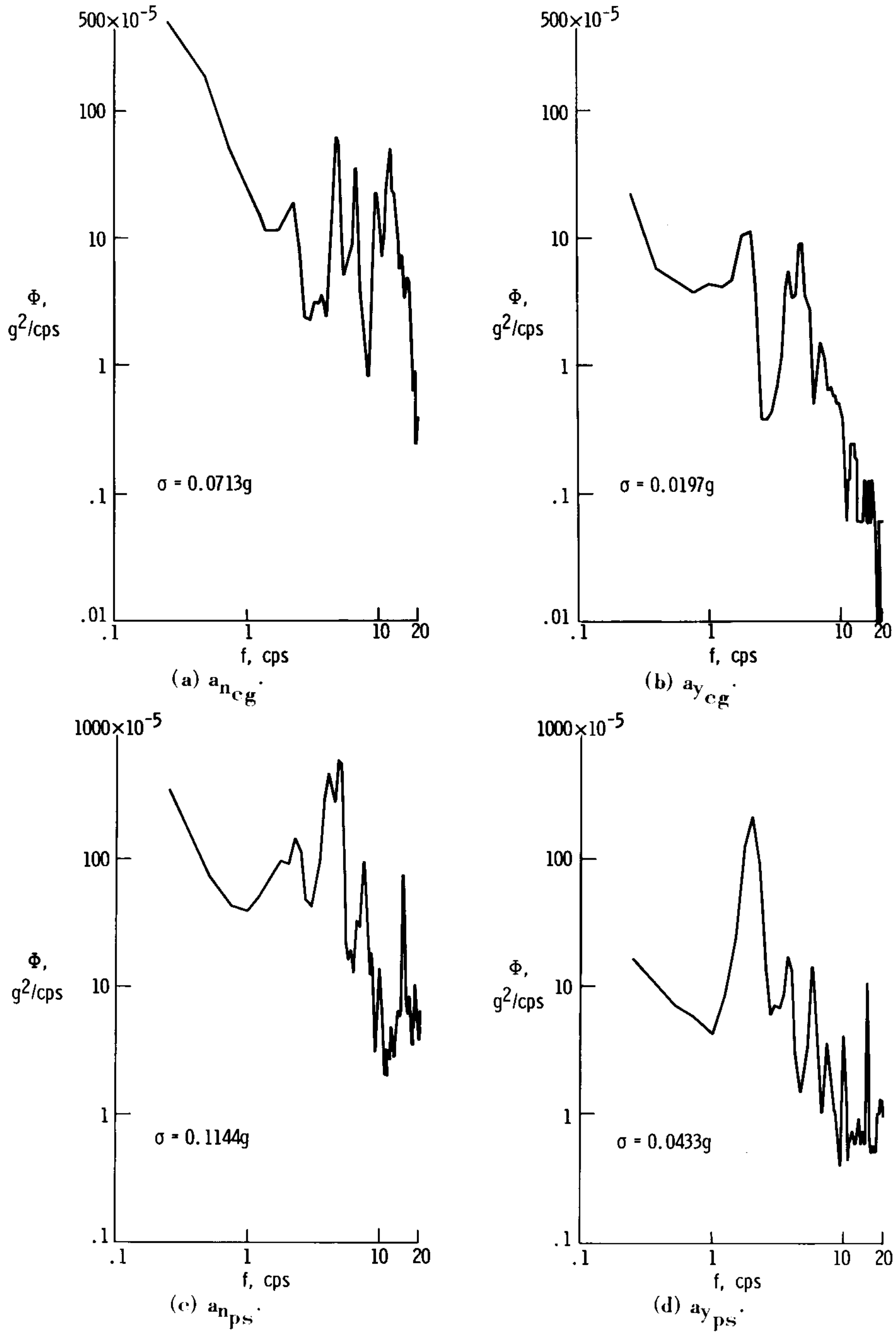

Figure 6.— Power spectra of XB-70 airplane response to turbulence with flight augmentation control system on. $M = 2.4$; $h = 55,000$ ft (16,764 m); $W = 410,000$ lb (208,787 kg); 40-second sample.

The normal-acceleration center-of-gravity response in figure 6(a) shows that the response is primarily in the rigid-body longitudinal short-period mode (0.2 cps). The response in the first structural mode is smaller than might be expected from the mode deflection shape. The low response may be due to the damping associated with the large wing motion in this mode. The results also show that there is response in the structural modes higher than the fourth mode, particularly near 12 cycles per second. From available data, it is not possible to determine the structural modes associated with the higher frequencies.

The lateral-acceleration response at the center of gravity shown in figure 6(b) is considerably less than the normal-acceleration response at the center of gravity, as would be expected. Although structural modes are not predominant in the lateral response, the data show that several structural modes less than 8 cps are present in the total response.

The normal-acceleration response at the pilot's station shown in figure 6(c) is due primarily to the lowest four structural modes, with most of the response associated with the third and fourth modes. Higher modes are contributing to the response at 7.5 cps and 15 cps. The relatively large response in the higher modes is probably associated with the large modal amplitude of the forward fuselage and the low aerodynamic damping that would be expected from the relatively small wing motion in these modes.

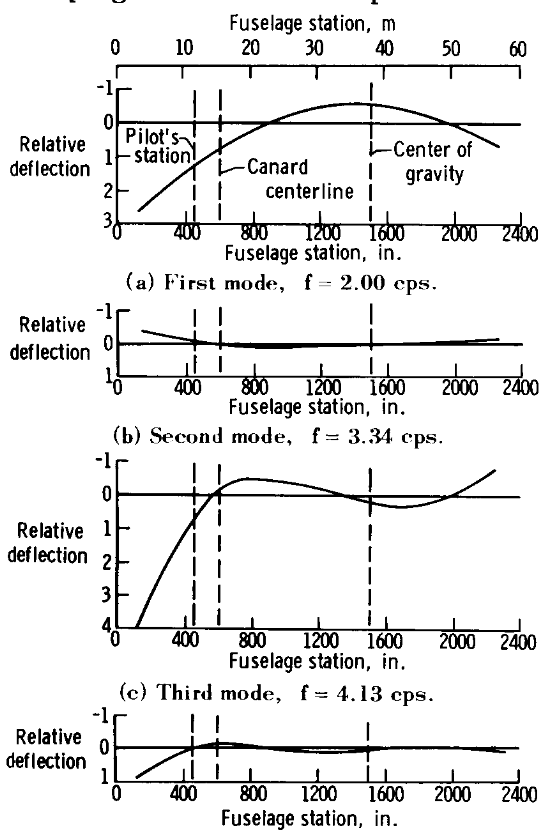

(a) First mode, f = 2.00 cps.

(b) Second mode, f = 3.34 cps.

(c) Third mode, f = 4.13 cps.

(d) Fourth mode, f = 5.70 cps.

Figure 7.— Calculated fuselage deflection (normalized to unit wing-tip deflection) for first four symmetrical modes of the XB-70 airplane, adapted from reference 10. Median weight; wing-tip deflection of 65°.

In figure 6(d), the lateral-acceleration response at the pilot's station is almost entirely due to a fuselage side-bending mode at 2 cps. Response of higher side-bending modes is indicated, but these modes contribute very little to the overall response.

As an aid in interpreting the response, the lowest four symmetrical modes, obtained from reference 10, are shown in figures 7(a) to 7(d). The mode shapes and frequencies were not calculated for the flight conditions analyzed, and, hence, exact correlation with measured response would not be expected. These modes and frequencies were calculated for a median weight condition which approximates the weight condition for the flight data. The location of the accelerometers at the pilot's station and the center of gravity and the location of the canard centerline are indicated for reference.

As mentioned previously, the effect of aerodynamic damping associated with a given structural mode can affect the response in that mode and, hence, affect the acceleration response at a given station. However, the contribution of a given mode to the overall response at a given station is also strongly dependent on the proximity of the node point. Figure 7 shows that the forward node points of the upper three modes are very close to the pilot's station for the conditions used in the calculations. Any change in the airplane mass distribution (fuel usage, for example) would alter these mode shapes and affect the modal response at the pilot's station. However, the actual mode deflection shapes are not known for the flight condition analyzed; thus, the effect of the node-point locations on the response of the pilot's station cannot be determined.

The average number of accelerations per second of flight that exceeded given values of acceleration is shown in figure 8 for the 40-second data sample used in figure 6. For this sample, the maximum normal acceleration at the center of gravity was $\Delta g = 0.35$ and at the pilot's station, $\Delta g = 0.50$. The maximum lateral accelerations measured were $\Delta g = 0.10$ at the center of gravity and $\Delta g = 0.15$ at the pilot's station.

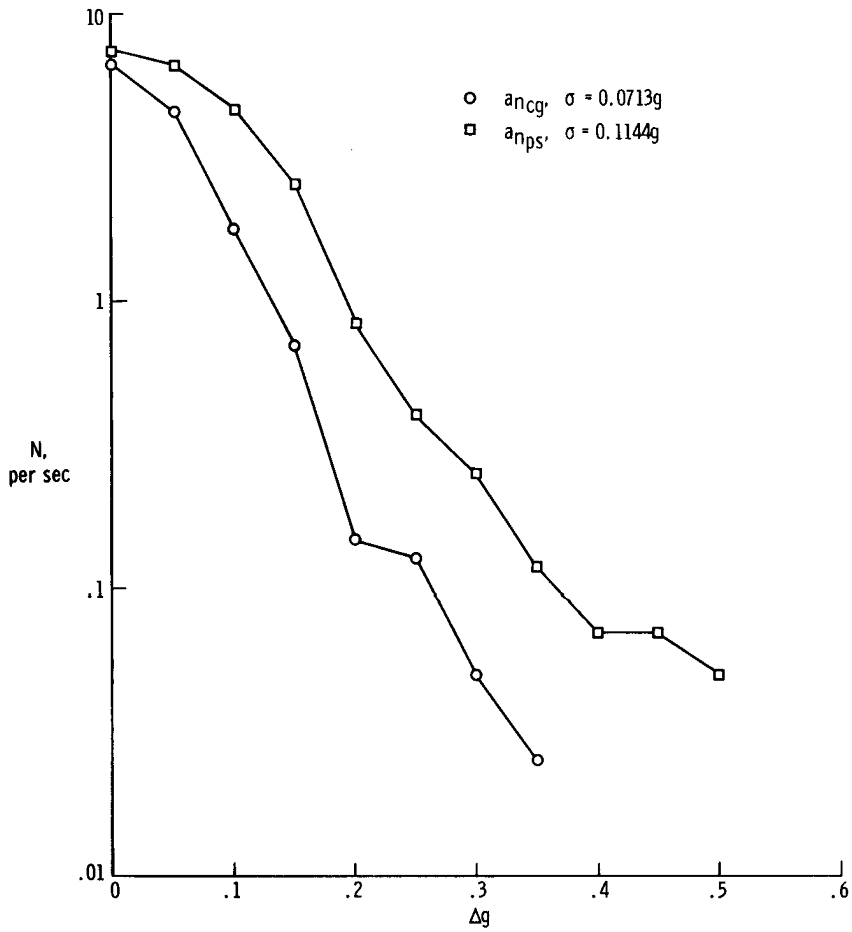

Figure 8.— Average number of crossings with positive slopes for a given acceleration level. M = 2.4; h = 55,000 ft (16,764 m); W = 410,000 lb (208,787 kg).

Probability densities of normal acceleration for each location are presented in figure 9 along with the Gaussian curves corresponding to the σ value measured for each sample. Application of the χ^2 goodness-of-fit test shows that the experimental probability density is not equivalent to the normal density function.

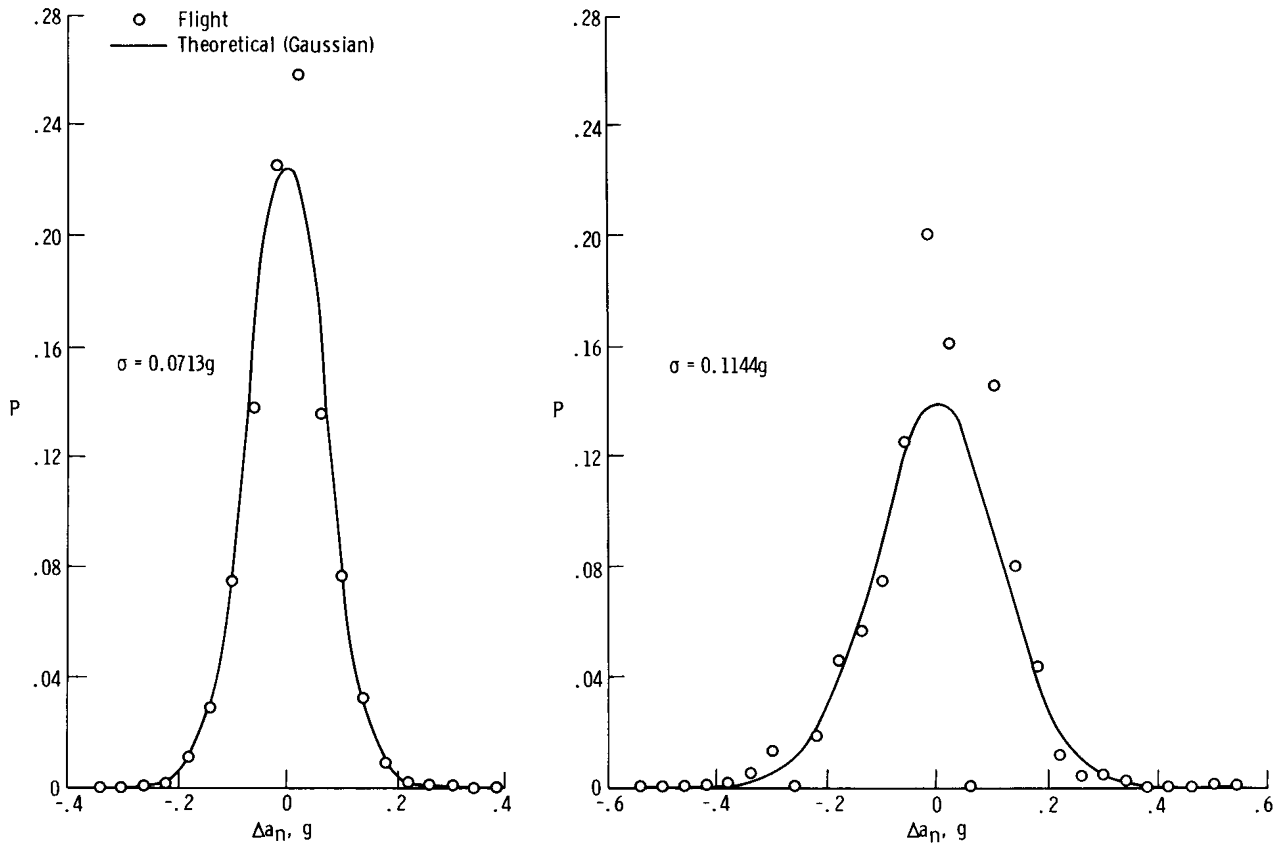

(a) Center of gravity.

(b) Pilot station.

Figure 9.– Probability density of measured normal accelerations. M = 2.4; h = 55,000 ft (16,764 m); W = 410,000 lb (208,787 kg).

CONCLUDING REMARKS

A preliminary investigation of the dynamic response of the XB-70 airplane on 96 flights has provided information on the amount of turbulence encountered at altitudes above 40,000 feet (12,192 meters) at supersonic speeds and on the nature of the aircraft structural response to turbulence. The data cover operations of the two XB-70 airplanes over the western portion of the United States. In general, the results for 75,757 miles (121,919 kilometers) of operation at altitudes above 40,000 feet (12,192 meters) at supersonic speeds show that the XB-70 encountered turbulence an average of 7.2 percent of the miles flown between 40,000 feet (12,192 meters) and 65,000 feet (19,812 meters) and an average of 3.3 percent of the miles above 65,000 feet (19,812 meters). The probability of exceeding a given length of turbulence decreases rapidly with increasing length, with less than 1 percent of the turbulent areas exceeding 100 miles (160.93 meters).

Power-spectral-density estimates of the acceleration response to turbulence at the airplane center of gravity and at the pilot's station show that the response of structural modes contributes an appreciable amount to the total response, particularly at the pilot's station.

Flight Research Center,
National Aeronautics and Space Administration,
Edwards, Calif., July 6, 1967,
732-01-00-03-24.

APPENDIX A

SYMBOLS

a_n	normal acceleration, g
a_{n_s}	reference normal acceleration, $\frac{m\rho_o S V_e U}{2W}$, g
a_y	lateral acceleration, g
$C_{L_g}(s)$	transient lift response to penetration of sharp-edge gust
$C_{L_\alpha}(s)$	transient lift response to unit-step change in angle of attack
c	reference wing chord, feet (meters)
f	frequency, cycles per second
g	acceleration due to gravity, feet/second^2 (meters/second^2)
H	gust-gradient distance (horizontal distance from zero to maximum gust velocity), chords
h	pressure altitude, feet (meters)
K_g	gust factor
M	Mach number
m	wing lift-curve slope, per radian
N	average number of crossings with positive slopes
P	probability density of acceleration
S	wing area, feet^2 (meters^2)
s	distance of penetration into gust, chords
s_1	dummy variable in superposition integral, chords
U	gust velocity, maximum value, feet/second (meters/second)
U_{de}	derived gust velocity, feet/second (meters/second)

$u(s)$	gust velocity, feet/second (meters/second)
V_e	equivalent airspeed, feet/second (meters/second)
W	airplane weight, pounds (kilograms)
Δg	incremental acceleration
μ_g	airplane mass ratio, $\frac{2W}{\rho c m g S}$
ρ	air density, slugs/foot^3 (kilograms/meter^3)
ρ_o	air density at sea level, slugs/foot^3 (kilograms/meter^3)
σ	root mean square
Φ	power spectral density

Subscripts:

cg	center of gravity
ps	pilot station
max	maximum

APPENDIX B

CALCULATED GUST FACTOR FOR A DELTA WING

In order to define the threshold of airplane response in terms of a derived gust velocity threshold, the analysis of reference 7 was extended to include a low-aspect-ratio delta wing for subsonic and high-supersonic speeds.

If the airplane is restricted to vertical displacement, the equation of motion for a rigid airplane at constant forward velocity can be written as (see ref. 7)

$$\frac{a_n(s)}{a_{n_S}} + \frac{1}{\mu_g}\int_0^s \frac{1}{m} C_{L_\alpha}(s - s_1)\frac{a_n(s_1)}{a_{n_S}}\,ds_1 = \int_0^s \frac{1}{m} C_{L_g}(s - s_1)\left(\frac{\pi}{H}\sin\frac{\pi s_1}{2H}\cos\frac{\pi s_1}{2H}\right)ds_1 \tag{A1}$$

where

$$a_{n_S} = \frac{m\rho_o S V_e U}{2W}$$

$$\mu_g = \frac{2W}{\rho c m g S}$$

In this expression, the gust velocity has been taken as $\frac{u(s)}{U} = \sin^2\frac{\pi s}{2H}$.

Equation (A1) was solved for histories of the acceleration ratio for subsonic speeds by using the transient lift functions for wings of finite span in incompressible flow from reference 11 and for supersonic speeds for a delta wing with supersonic leading edge by using the transient lift functions from reference 12. The results of the calculations were used to determine the gust factor K_g, defined as

$$K_g = \left(\frac{a_n}{a_{n_S}}\right)_{max} \tag{A2}$$

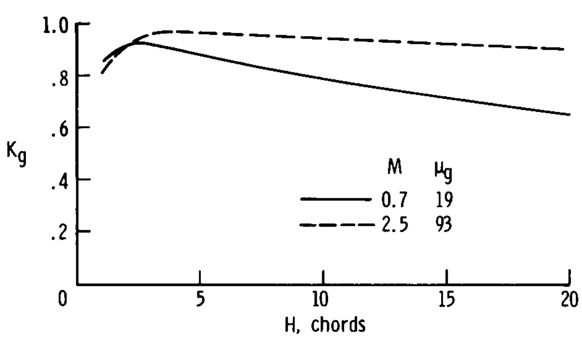

Figure 10.– Variation of gust factor with gust-gradient distance. W = 350,000 lb (158,756 kg).

Since K_g is dependent on the values of both H and μ_g, the solutions of equation (A1) were carried out for a range of values of both parameters. The variation of K_g with H for one value of airplane weight and for M = 0.7 and M = 2.5 is shown, for example, in figure 10. Results of these calculations were used as a guide in determining the

Δg threshold for the acceleration response at the airplane center of gravity by using the expression

$$\left(U_{de}\right)_{max} = \frac{2a_n W}{m\rho_o S V_e K_g} \tag{A3}$$

with K_g chosen for a gust-gradient distance of 12.5 chords.

REFERENCES

1. Houbolt, John C.; Steiner, Roy; and Pratt, Kermit G.: Dynamic Response of Airplanes to Atmospheric Turbulence Including Flight Data on Input and Response. NASA TR-R-199, 1964.

2. Coleman, Thomas L.; and Steiner, Roy: Atmospheric Turbulence Measurements Obtained From Airplane Operations at Altitudes Between 20,000 and 75,000 Feet for Several Areas in the Northern Hemisphere. NASA TN D-548, 1960.

3. Crooks, Walter: High Altitude Clear Air Turbulence. Tech. Rep. AFFDL-TR-65-144, Wright-Patterson AFB, U.S. Air Force, Sept. 1965.

4. Mechtly, E. A.: The International System of Units - Physical Constants and Conversion Factors. NASA SP-7012, 1964.

5. Andrews, William H.: Summary of Preliminary Data Derived From the XB-70 Airplanes. NASA TM X-1240, 1966.

6. Richardson, Norman R.: NACA VGH Recorder. NACA TN 2265, 1951.

7. Pratt, Kermit G.; and Walker, Walter G.: A Revised Gust-Load Formula and a Reevaluation of V-G Data Taken on Civil Transport Airplanes From 1933 to 1950. NACA Rept. 1206, 1954.

8. Anon.: U.S. Standard Atmosphere, 1962. NASA, U.S. Air Force, and U.S. Weather Bur., Dec. 1962.

9. Press, Harry; and Tukey, John W.: Power Spectral Methods of Analysis and Their Application to Problems in Airplane Dynamics. Vol. IV of AGARD Flight Test Manual, Pt. IVC, Enoch J. Durbin, ed., June 1956, pp. IVC: 1-IVC: 41.

10. Wykes, John H.; and Mori, Alva S.: An Analysis of Flexible Aircraft Structural Mode Control. Tech. Rep. AFFDL-TR-65-190, Part I, Wright-Patterson AFB, U.S. Air Force, June 1966.

11. Drischler, Joseph A.: Approximate Indicial Lift Functions for Several Wings of Finite Span in Incompressible Flow as Obtained From Oscillatory Lift Coefficients. NACA TN 3639, 1956.

12. Miles, John W.: Transient Loading of Wide Delta Airfoils at Supersonic Speeds. J. Aeron. Sci., vol. 18, no. 8, Aug. 1951, pp. 543-554.

TABLE I. – GEOMETRIC CHARACTERISTICS OF THE XB-70 AIRPLANE

Total wing –		
Total area (includes 2482.34 ft^2 (230.62 m^2) covered by fuselage but not 33.53 ft^2 (3.12 m^2) of the wing ramp area), ft^2 (m^2)	6297.8	(585.07)
Span, ft (m)	105	(32)
Aspect ratio		1.751
Taper ratio		0.019
Dihedral angle, deg:		
XB-70-1		0
XB-70-2		5
Root chord (wing station 0), ft (m)	117.76	(35.89)
Tip chord (wing station 630 in. (16 m)), ft (m)	2.19	(0.67)
Mean aerodynamic chord (wing station 213.85 in. (5.43 m)), in. (m)	942.38	(23.94)
Fuselage station of 25-percent wing mean aerodynamic chord, in. (m)	1621.22	(41.18)
Sweepback angle, deg:		
Leading edge		65.57
25-percent element		58.79
Trailing edge		0
Incidence angle, deg:		
Root (fuselage juncture)		0
Tip (fold line and outboard)		-2.60
Airfoil section:		
Root to wing station 186 in. (4.72 m) (thickness-chord ratio, 2 percent)		0.30 to 0.70 HEX (MOD)
Wing station 460 in. (11.68 m) to 630 in. (16 m) (thickness-chord ratio, 2.5 percent)		0.30 to 0.70 HEX (MOD)
Inboard wing –		
Area (includes 2482.34 ft^2 (230.62 m^2) covered by fuselage but not 33.53 ft^2 (3.12 m^2) wing ramp area), ft^2 (m^2)	5256.0	(488.28)
Span, ft (m)	63.44	(19.34)
Aspect ratio		0.766
Taper ratio		0.407
Dihedral angle, deg:		
XB-70-1		0
XB-70-2		5
Root chord (wing station 0), ft (m)	117.76	(35.89)
Tip chord (wing station 380.62 in. (9.67 m)), ft (m)	47.94	(14.61)
Mean aerodynamic chord (wing station 163.58 in. (4.15 m)), in. (m)	1053	(26.75)
Fuselage station of 25-percent wing mean aerodynamic chord, in. (m)	1538.29	(39.07)
Sweepback angle, deg:		
Leading edge		65.57
25-percent element		58.79
Trailing edge		0
Airfoil section:		
Root (thickness-chord ratio, 2 percent)		0.30 to 0.70 HEX (MOD)
Tip (thickness-chord ratio, 2.4 percent)		0.30 to 0.70 HEX (MOD)

TABLE I. – GEOMETRIC CHARACTERISTICS OF THE XB-70 AIRPLANES - Continued

Mean camber (leading edge), deg:		
Butt plane 0		0.15
Butt plane 107 in. (2.72 m)		4.40
Butt plane 153 in. (3.89 m):		
XB-70-1		3.15
XB-70-2		2.75
Butt plane 257 in. (6.53 m):		
XB-70-1		2.33
XB-70-2		2.60
Butt plane 367 in. (9.32 m) to tip		0
Outboard wing –		
Area (one side only), ft^2 (m^2)	520.90	(48.39)
Span, ft (m)	20.78	(6.33)
Aspect ratio		0.829
Taper ratio		0.046
Dihedral angle, deg:		
XB-70-1		0
XB-70-2		5
Root chord (wing station 380.62 in. (9.67 m)), ft (m)	47.94	(14.61)
Tip chord (wing station 630 in. (16.00 m)), ft (m)	2.19	(0.67)
Mean aerodynamic chord (wing station 467.37 in. (11.87 m)), in. (m)	384.25	(9.76)
Sweepback angle, deg:		
Leading edge		65.57
25-percent element		58.79
Trailing edge		0
Airfoil section:		
Root (thickness-chord ratio, 2.4 percent)		0.30 to 0.70 HEX (MOD)
Tip (thickness-chord ratio, 2.5 percent)		0.30 to 0.70 HEX (MOD)
Down deflection from wing reference plane, deg:		
XB-70-1		0, 25, 65
XB-70-2		0, 30, 70
Skewline of tip fold, deg:		
Leading edge in		1.5
Leading edge down		3

Wing-tip area in wing reference plane (one side only), ft^2 (m^2):

	XB-70-1	XB-70-2		
Rotated down	25°	30°	472.04	(43.85)
Rotated down	65°	70°	220.01	(20.44)

	Wing tips Up		Wing tips Down	
Elevons (data for one side):				
Total area aft of hinge line, ft^2 (m^2)	197.7	(18.37)	135.26	(12.57)
Span, ft (m)	20.44	(6.23)	13.98	(4.26)
Inboard chord (equivalent), in. (m)	116	(2.95)	116	(2.95)
Outboard chord (equivalent), in. (m)	116	(2.95)	116	(2.95)
Sweepback angle of hinge line, deg		0		0
Deflection, deg:				
As elevator				-25 to 15
As aileron with elevators at ±15° or less				-15 to 15
As aileron with elevators at -25°				-5 to 5
Total				-30 to 30

TABLE I. – GEOMETRIC CHARACTERISTICS OF THE XB-70 AIRPLANES - Continued

Canard –		
Area (includes 150.31 ft^2 (13.96 m^2) covered by fuselage), ft^2 (m^2)	415.59	(38.61)
Span, ft (m)	28.81	(8.78)
Aspect ratio		1.997
Taper ratio		0.388
Dihedral angle, deg		0
Root chord (canard station 0), ft (m)	20.79	(6.34)
Tip chord (canard station 172.86 in. (4.39 m)), ft (m)	8.06	(2.46)
Mean aerodynamic chord (canard station 73.71 in. (1.87 m)), in. (m)	184.3	(4.68)
Fuselage station of 25-percent canard mean aerodynamic chord, in. (m)	553.73	(14.06)
Sweepback angle, deg:		
Leading edge		31.70
25-percent element		21.64
Trailing edge		-14.91
Incidence angle (nose up), deg		0 to 6
Airfoil section:		
Root (thickness-chord ratio 2.5 percent)		0.34 to 0.66 HEX (MOD)
Tip (thickness-chord ratio 2.52 percent)		0.34 to 0.66 HEX (MOD)
Ratio of canard area to wing area		0.066
Canard flap (one of two):		
Area (aft of hinge line), ft^2 (m^2)	54.69	(5.08)
Ratio of flap area to canard semi-area		0.263
Vertical tail (one of two) –		
Area (includes 8.96 ft^2 (0.83 m^2) blanketed area), ft^2 (m^2)	233.96	(21.74)
Span, ft (m)	15	(4.57)
Aspect ratio		1
Taper ratio		0.30
Root chord (vertical-tail station 0), ft (m)	23.08	(7.03)
Tip chord (vertical-tail station 180 in. (4.57 m)), ft (m)	6.92	(2.11)
Mean aerodynamic chord (vertical-tail station 73.85 in. (1.88 m)), in. (m)	197.40	(5.01)
Fuselage station of 25-percent vertical-tail mean aerodynamic chord, in. (m)	2188.50	(55.59)
Sweepback angle, deg:		
Leading edge		51.77
25-percent element		45
Trailing edge		10.89
Airfoil section:		
Root (thickness-chord ratio 3.75 percent)		0.30 to 0.70 HEX (MOD)
Tip (thickness-chord ratio 2.5 percent)		0.30 to 0.70 HEX (MOD)
Cant angle, deg		0
Ratio vertical tail to wing area		0.037
Rudder travel, deg:		
With gear extended		±12
With gear retracted		±3

TABLE I. – GEOMETRIC CHARACTERISTICS OF THE XB-70 AIRPLANES - Concluded

Fuselage (includes canopy) –		
Length, ft (m)	185.75	(56.62)
Maximum depth (fuselage station 878 in. (22.30 m)), in. (m)	106.92	(2.72)
Maximum breadth (fuselage station 855 in. (21.72 m)), in. (m)	100	(2.54)
Side area, ft^2 (m^2)	939.72	(87.30)
Planform area, ft^2 (m^2)	1184.78	(110.07)
Center of gravity:		
Forward limit, percent mean aerodynamic chord		19.0
Aft limit, percent mean aerodynamic chord		25.0
Duct –		
Length, ft (m)	104.84	(31.96)
Maximum depth (fuselage station 1375 in. (34.93 m)), in. (m)	90.75	(2.31)
Maximum breadth (fuselage station 2100 in. (53.34 m)), in. (m)	360.70	(9.16)
Side area, ft^2 (m^2)	716.66	(66.58)
Planform area, ft^2 (m^2)	2342.33	(217.61)
Inlet captive area (each), $in.^2$ (m^2)	5600	(3.61)
Surface areas (net wetted), ft^2 (m^2):		
Fuselage and canopy	2871.24	(266.75)
Duct	4956.66	(460.49)
Wing, wing tips, and wing ramp	7658.44	(711.49)
Vertical tails (two)	936.64	(87.02)
Canard	530.83	(49.32)
Tail pipes	340.45	(31.62)
Total	17,294.26	(1606.69)
Engines	6 YJ93-GE-3	